Functional Models for Vanadium Haloperoxidase: Reactivity and Mechanism of Halide Oxidation

Gerard J. Colpas, Brent J. Hamstra, Jeff W. Kampf, and Vincent L. Pecoraro*

Contribution from the Department of Chemistry, University of Michigan, Ann Arbor, Michigan 48109-1055

Received November 13, 1995[⊗]

Abstract: A series of oxoperoxovanadium(V) complexes (ligands: H_3nta = nitrilotriacetic acid, H_3heida = *N*-(2-hydroxyethyl)iminodiacetic acid, H_2ada = *N*-(2-amidomethyl)iminodiacetic acid, Hbpg = *N*,*N*-bis(2-pyridylmethyl)-glycine, and tpa = *N*,*N*,*N*-tris(2-pyridylmethyl)amine) were characterized as functional models for the vanadium haloperoxidase enzymes. The crystal structures of K[$VO(O_2)$Hheida], K[$VO(O_2)$ada], [$VO(O_2)$bpg], and H[$VO(O_2)$bpg]$_2(ClO_4)$ were obtained. These complexes all possess a distorted pentagonal bipyramidal coordination sphere containing a side-on bound peroxide. In the presence of sufficient acid equivalents these complexes catalyze the two-electron oxidation of bromide or iodide by peroxide. Halogenation of an organic substrate was demonstrated by following the visible conversion of Phenol Red to Bromophenol Blue. In the absence of substrate, dioxygen can be generated by the halide-assisted disproportionation of hydrogen peroxide. In addition, some of these complexes can efficiently catalyze the peroxidative halogenation reaction, performing multiple turnovers in minutes. The kinetic analysis of the halide oxidation reaction indicates a mechanism which is first order in protonated peroxovanadium complex and halide. The bimolecular rate constants for both bromide and iodide oxidation were determined, with the iodide rates being approximately 5−6 times faster than the bromide rates. The rate constants obtained for bromide oxidation range from a maximum of 280 M^{-1} s^{-1} for the Hheida complex to a minimum of 21 M^{-1} s^{-1} for the Hbpg complex. The pK_a of activation for each complex in acetonitrile was determined to range from 5.4 to 6.0. On the basis of the chemistry observed for these model compounds, a mechanism of halide oxidation and a detailed catalytic cycle are proposed for the vanadium haloperoxidase enzyme.

Introduction

While isolation of the vanadium haloperoxidase (VHPO) from the marine algae *Ascophyllum nodosum* in 1984 provided the first example of a vanadium-dependent enzyme,[1,2] it is now apparent that these vanadoproteins are found in most marine algae, seaweed, and some lichens.[3] Haloperoxidases isolated from different sources are characterized as iodoperoxidases, bromoperoxidases, or chloroperoxidases,[4] depending on the most electronegative halogen the enzyme is capable of oxidizing. VHPOs are thought to be involved in the production of a large quantity of halogenated organics *in vivo*.[5] Recent work has shown that VHPO has the ability to selectively halogenate particular substrates at specific locations on the phenyl ring.[6] These compounds include a number with potent antifungal, antibacterial, and antitumor properties.[7]

In the absence of an organic substrate, oxygen is generated by a halide-assisted disproportionation of hydrogen peroxide.[8] In the presence of bromide, this was shown to be singlet oxygen.[9] A slight pH dependence has been observed for these "catalase" and haloperoxidase reactions, with halogenation favored at lower pH and oxygen production favored at higher pH.[10]

The VHPOs require 1 equiv of vanadium for activity.[11] The vanadium center does not appear to undergo redox cycling during turnover and is proposed to function as a Lewis acid, differing from the more common heme-containing enzymes that appear to form ferryl intermediates during catalysis.[12] The oxidized (vanadate) form of the enzyme will not turn over without added hydrogen peroxide.[13] The reduced (vanadyl) form of the enzyme is inactive and is not reactivated by addition of peroxide and/or bromide.[14] No evidence has been presented to suggest that a V(III) form of the enzyme exists.

Extended X-ray absorption fine structure (EXAFS) analysis of the active site indicates the presence of an oxovanadium(V) with N/O donor ligands.[15−17] Recently, a crystallographic study on an oxidized form of vanadium chloroperoxidase described a five-coordinate trigonal bipyramidal vanadium(V) atom coordinated by one histidine nitrogen, three oxo donors, and an azide.[18] This chloroperoxidase is shown to have strong

[⊗] Abstract published in *Advance ACS Abstracts,* March 15, 1996.

(1) Vilter, H. *Bot. Mar.* **1983**, *26*, 451−455.
(2) Vilter, H. *Phytochemistry* **1984**, *23*, 1387−1390.
(3) Wever, R.; Krenn, B. E. Vanadium Haloperoxidases In *Vanadium in Biological Systems*; Chasteen, N. D., Ed.; Kluwer Academic Publishers: Dordrecht, 1990; pp 81−97.
(4) Soedjak, H. S.; Butler, A. *Inorg. Chem.* **1990**, *29*, 5015−5017.
(5) Neidleman, S. L.; Geigert, J. L. *Biohalogenation*; Ellis Horwood Ltd. Press: New York, 1986.
(6) Tschirret-Guth, R. A.; Butler, A. *J. Am. Chem. Soc.* **1994**, *116*, 411−412.
(7) Butler, A.; Walker, J. V. *Chem. Rev.* **1993**, *93*, 1937−1944.
(8) Everett, R. R.; Butler, A. *Inorg. Chem.* **1989**, *28*, 393−395.
(9) Everett, R. R.; Soedjak, H. S.; Butler, A. *J. Biol. Chem.* **1990**, *265*, 15671−15679.
(10) Everett, R. R.; Kanofsky, J. R.; Butler, A. *J. Biol. Chem.* **1990**, *265*, 4908−4914.
(11) de Boer, E.; van Kooyk, Y.; Tromp, M.; Wever, R. *Biochim. Biophys. Acta* **1986**, *869*, 48−53.
(12) Dawson, J. H. *Science* **1988**, *240*, 433−439.
(13) Tromp, M.; Olafsson, G.; Krenn, B.; Wever, R. *Biochim. Biophys. Acta* **1990**, *1040*, 192−198.
(14) de Boer, E.; Koon, K.; Wever, R. *Biochemistry* **1988**, *27*, 1629−1635.
(15) Arber, J. M.; de Boer, E.; Garner, C. D.; Hasnain, S. S.; Wever, R. *Biochemistry* **1989**, *28*, 7968−7973.
(16) Hormes, J.; Kuetgens, U.; Chauvistre, R.; Schriber, W.; Anders, N.; Vilter, H.; Rehder, D.; Weidemann, C. *Biochim. Biophys. Acta* **1988**, *956*, 293−299.
(17) Weidemann, C.; Rehder, D.; Kuetgens, U.; Hormes, J.; Vilter, H. *Chem.Phys.* **1989**, *136*, 405−412.
(18) Messerschmidt, A.; Wever, R. *Proc. Natl. Acad. Sci. U.S.A.* **1996**, *93*, 392−396.

0002-7863/96/1518-3469$12.00/0

sequence homology with the vanadium bromoperoxidase isolated from algae for the amino acid residues located near to the vanadium binding site.[19]

Spectroscopic and kinetic studies support the formation of peroxovanadium intermediates. Under conditions of increased hydrogen peroxide concentration, X-ray absorption near-edge structure (XANES) measurements are consistent with a peroxide binding to the vanadium(V) which is reversed upon addition of bromide.[20] Reactivity studies are consistent with an ordered mechanism requiring hydrogen peroxide and then halide.[21] While kinetic studies indicate that both the halogenation and disproportionation reactions proceed through a common intermediate, proposed to be an oxidized halogen species,[22] the exact composition of the active oxidizing agent and active halogenating intermediate are unknown.

Vanadate in acidic aqueous solution has been shown to catalyze the oxidation of both iodide and bromide by hydrogen peroxide.[23,24] The oxidized bromine species can then halogenate an organic substrate or react with a second equivalent of hydrogen peroxide to generate dioxygen. Kinetic analysis of the oxidation of bromide showed that a triperoxodivanadate species is the active catalyst.[25] Two vanadium(V) Schiff base complexes were shown to catalyze bromination reactions using hydrogen peroxide in DMF solution.[26] These halogenation reactions were found to be stoichiometric in acid equivalents added. Recently, we reported a structurally characterized oxoperoxovanadium(V) complex which acts as a functional model of VHPO, which catalyzed the rapid and stoichiometric halogenation of an organic substrate or the generation of dioxygen.[27]

Herein we report a series of related oxoperoxovanadium complexes that are functional models for the VHPO enzymes. The ligands employed are derivatized tripodal-amine chelates which form stable oxoperoxovanadium complexes (Figure 1). These complexes have reactivity modeling the enzymes' activity and are being used to understand the chemical mechanisms employed in the catalytic cycle, including halide oxidation, the halogenation of organic compounds, and the halide-assisted disproportionation of hydrogen peroxide.

Experimental Section

The following ligand abbreviations are used throughout the text: H_3nta = nitrilotriacetic acid, H_3heida = *N*-(2-hydroxyethyl)iminodiacetic acid, H_2ada = *N*-(2-amidomethyl)iminodiacetic acid, Hbpg = *N*,*N*-bis(2-pyridylmethyl)glycine, and tpa = *N*,*N*,*N*-tris(2-pyridylmethyl)-amine.

Vanadium(V) oxide, nitrilotriacetic acid, *N*-(2-amidomethyl)iminodiacetic acid, iminodiacetic acid, 2-picolyl chloride hydrochloride, 2-pyridinecarboxaldehyde, 2-(aminomethyl)pyridine, ethyl bromoacetate and Phenol Red were purchased from Aldrich Chemical Co. *N*-(2-Hydroxyethyl)iminodiacetic acid was purchased from TCI America.

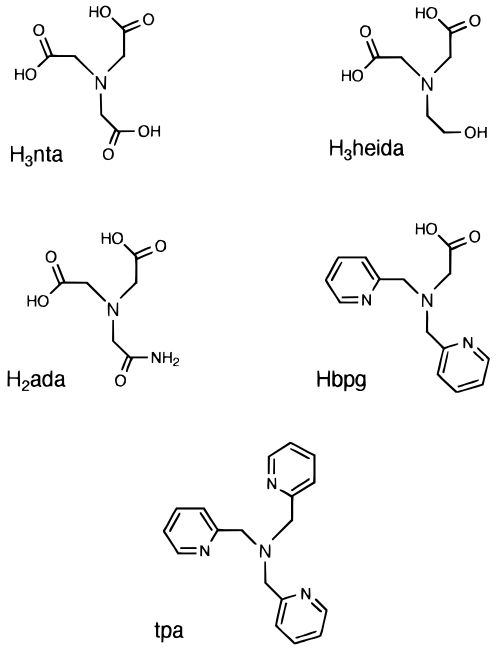

Figure 1. Ligands used in this study. The key to abbreviations is found in the Experimental Section.

All other reagents and solvents were reagent grade or better. Isotopically substituted hydrogen peroxide was generated from ^{18}O-enriched dioxygen (99%) purchased from Isotec Inc.

Preparation of Compounds. K_2[VO(O_2)nta] (**1**),[28] K_2[VO_2(nta)],[29] Hbpg·2HBr,[30] and tpa·3$HClO_4$[31] were synthesized by modifications of literature methods. Potassium vanadate was generated *in situ* by reaction of V_2O_5 with 2 equiv of KOH in aqueous solution. **CAUTION:** *Perchlorates are an explosion hazard and should be generated only when absolutely necessary and only in small quantities.*

K[VO(O_2)Hheida] (2). Potassium vanadate (5 mmol) in 20 mL of H_2O solution was stirred at 0 °C. The ligand (0.89 g, 5 mmol) was added with stirring until dissolved, and then 2 mL of 30% aqueous hydrogen peroxide was added dropwise to give a clear red-orange solution. The pH of this solution was adjusted to near 4 with concentrated HCl. The solution was stirred overnight and then kept at 5 °C for a few days. Ethanol (approximately 20 mL) was added until the solution appeared cloudy, and the solution was returned to the refrigerator. The orange crystals were collected the next day by filtration, washed with cold ethanol, and air-dried. Yield = 0.83 g (51%). Anal. Calcd (found) for $C_6H_9NO_8VK·H_2O$ (MW 331.2): C, 21.76 (21.61); H, 3.35 (3.11); N, 4.23 (4.32). ^{51}V NMR (H_2O): −565 ppm. ^{13}C NMR (D_2O): 183.2, 68.8, 64.9, 59.9 ppm. IR: ν (C═O, s) 1610, (C—O, s) 1461, (V═O, s) 961, (O—O, s) 920, (V—O_2, s, as) 570 cm^{-1}.

K[VO(O_2)ada] (3). Potassium vanadate (5 mmol) in 30 mL of H_2O solution was stirred at 0 °C. The ligand (0.95 g, 5 mmol) was added with stirring until dissolved, and then 2 mL of 30% aqueous hydrogen peroxide was added dropwise to give a clear red-orange solution. The pH of this solution was adjusted to 4 with HCl. The solution was stirred overnight and kept at 5 °C for a few days. Orange crystals were collected by filtration after a few days, washed with cold ethanol, and air-dried. Yield = 1.11 g (56%). Anal. Calcd (found) for $C_6H_8N_2O_8VK·4H_2O$ (MW 398.2): C, 18.1 (18.2); H, 4.05 (3.90); N, 7.04 (6.93). ^{51}V NMR (H_2O): −551 ppm. ^{13}C NMR (D_2O): 182.3, 176.6, 70.7, 66.7 ppm. IR: ν (C═O, s) 1680, 1643, (C—O, s) 1382, (V═O, s) 955, (O—O, s) 924, (V—O_2, s, as) 572 cm^{-1}.

[VO(O_2)bpg] (4). Potassium vanadate (2 mmol) in 30 mL of H_2O solution was stirred at 0 °C. Two milliliters of 30% aqueous hydrogen peroxide was added, and then the ligand (0.88 g, 2 mmol) in 10 mL of

(19) Vilter, H. *Metal Ions in Biological Systems*; Sigel, H., Sigel, A., Eds.; Dekker: New York, 1995; Vol. 31, pp 326−362.
(20) Kusthardt, U.; Hedman, B.; Hodgson, K. O.; Hahn, R.; Vilter, H. *FEBS Lett.* **1993**, *329*, 5−8.
(21) de Boer, E.; Wever, R. *J. Biol. Chem.* **1988**, *263*, 12326−12332.
(22) Butler, A. Vanadium Bromoperoxidase In *Bioinorganic Catalysis*; Reedijk, J., Ed.; Marcel Dekker, Inc.: New York, 1993; pp 425−445.
(23) de la Rosa, R. I.; Clague, M. J.; Butler, A. *J. Am. Chem. Soc.* **1992**, *114*, 760−761.
(24) Secco, F. *Inorg. Chem.* **1980**, *19*, 2722−2725.
(25) Clague, M. J.; Butler, A. *J. Am. Chem. Soc.* **1995**, *117*, 3475−3484.
(26) Clague, M. J.; Keder, N. L.; Butler, A. *Inorg. Chem.* **1993**, *32*, 4754−4761.
(27) Colpas, G. J.; Hamstra, B. J.; Kampf, J. W.; Pecoraro, V. L. *J. Am. Chem. Soc.* **1994**, *116*, 3627−3628.
(28) Sivak, M.; Joniakova, D.; Schwendt, P. *Transition Met. Chem. (London)* **1993**, *18*, 304−308.
(29) Nishizawa, M.; Saito, K. *Inorg. Chem.* **1980**, *19*, 2284−2288.
(30) Cox, D. D.; Benkovic, S. J.; Bloom, L. M.; Bradley, F. C.; Nelson, M. J.; Que, L., Jr.; Wallick, D. E. *J. Am. Chem. Soc.* **1988**, *110*, 2026−2032.
(31) Anderegg, G.; Wenk, F. *Helv. Chim. Acta* **1967**, *50*, 2330−2332.

Table 1. Summary of Crystallographic Data for K[$VO(O_2)$Hheida]·H_2O (**2**) K[$VO(O_2)$ada]·H_2O (**3**) [$VO(O_2)$bpg]·H_2O (**4**) and H[$VO(O_2)$bpg]ClO_4 (**6**)

	2	**3**	**4**	**6**
formula	$C_6H_9N_1O_8VK·H_2O$	$C_6H_8N_2O_8VK·4H_2O$	$C_{14}H_{14}N_3O_5V·H_2O$	$C_{14}H_{14}N_3O_5V·0.5HClO_4·0.5C_3H_5N$
MW	329.18	398.24	373.24	432.99
cryst syst	monoclinic	monoclinic	monoclinic	monoclinic
space group	$P2_1/n$ (No. 14)	$P2_1/c$ (No. 14)	Cc (No. 9)	$C2/c$ (No. 15)
a, Å	6.740(2)	6.395(1)	15.310(3)	24.592(7)
b, Å	11.510(3)	10.395(3)	7.7883(2)	12.530(6)
c, Å	14.841(4)	21.352(7)	14.192(3)	12.553(3)
α, deg	90	90	90	90
β, deg	93.12(2)	91.94(2)	116.61(2)	92.854(8)
γ, deg	90	90	90	90
V, Å^3	1149.6(5)	1418.5(7)	1513.2(6)	3863(2)
Z	4	4	4	8
abs coeff (μ), cm^{-1}	13.12	10.33	6.94	6.26
cryst size, mm^3	0.20 × 0.24 × 0.28	0.12 × 0.20 × 0.32	0.24 × 0.28 × 0.30	0.48 × 0.16 × 0.20
2θ scan range, deg	5.5−55	5−55	5−60	5−52
temp, K	293	138	293	178
no. of unique data	2655	3274	2570	3796
no. of refined data	2655	3067	2569	3795
R/$R1$	0.0364[b]	0.0268[a]	0.0265[b]	0.0790[b]
R_w/wR^2	0.0674[d]	0.0408[c]	0.0687[d]	0.2356[d]
resd dens, e/Å^3	+0.24/−0.35	+0.44/−0.50	+0.33/−0.43	+1.09/−0.72

[a] $R = \sum(|F_o - F_c|)/\sum|F_o|$. [b] $R1 = \sum||F_o| - |F_c||/\sum|F_o|$. [c] $R_w = [\sum w(|F_o| - |F_c|)^2/\sum w|F_o|^2]^{1/2}$. [d] $wR^2 = [\sum w(F_o^2 - F_c^2)^2/\sum w(F_o^2)^2]^{1/2}$.

water was added dropwise. Precipitate formed almost immediately upon addition of the ligand. The solution was stirred for 6 h, after which the red-orange powder was collected by filtration, washed once with cold ethanol, and air-dried. Yield = 0.47 g (62%). Anal. Calcd (found) for $C_{14}H_{14}N_3O_5V·1.5H_2O$ (MW 382.2): C, 43.9 (43.8); H, 4.50 (4.68); N, 11.0 (10.9). ^{51}V NMR (CH_3CN): −543 ppm. ^{13}C NMR (CD_3CN): 178.1, 68.6, 158.1, 147.7, 141.9, 126.5, 124.4, 68.8 ppm. IR: ν (C═O, s) 1629, (C═C, s) 1611, (C−O, s) 1386, (V═O, s) 947, 933, (O−O, s) 910, (V−O_2, s, as) 571 cm^{-1}. This compound can be crystallized by evaporation of an acetonitrile solution at room temperature.

[$VO(O_2)$tpa]ClO_4 (5). Potassium vanadate (1 mmol) in 30 mL of H_2O solution was stirred at 0 °C. One milliliter of 30% aqueous hydrogen peroxide was added, and then the ligand (0.59 g, 1 mmol) in 10 mL of water was added dropwise. Aqueous concentrated potassium hydroxide solution was used to bring the pH to near 4, causing a precipitate to form almost immediately. The solution was stirred for 3 h, after which the red-orange powder was collected by filtration, washed once with cold ethanol, and air-dried. Yield = 0.28 g (54%). Anal. Calcd (found) for $C_{18}H_{18}N_4O_7VCl·2H_2O$ (MW 524.8): C, 41.2 (41.4); H, 4.23 (3.82); N, 10.7 (10.6). ^{51}V NMR (DMSO): −574 ppm. ^{13}C NMR (d_6-DMSO): 159.1, 147.1, 142.1, 125.8, 124.3, 67.8, 155.5, 146.1, 139.8, 123.8, 121.0, 64.4 ppm. IR: ν (C═C, s) 1607, (V═O, s) 948, (O−O, s) 904, (V−O_2, s, as) 580, (ClO_4, s) 1089 cm^{-1}.

H[$VO(O_2)$bpg]$_2$(ClO_4) (6). A slurry of **4** (0.39 g 1 mmol) was stirred in 100 mL of acetonitrile/proprionitrile (1/1). Upon completion of the dropwise addition of 0.1 mL of concentrated perchloric acid (1.1 mmol), the compound dissolved to give a clear red-orange solution. This solution was stirred for 1 h and then stored at −70 °C, yielding red-orange crystals after several days. Yield = 0.34 g (38%). Anal. Calcd (found) for $C_{28}H_{28}N_6O_{14}V_2Cl·C_3H_5N·C_2H_3N$ (MW 893.1): C, 43.6 (43.4); H, 3.97 (4.11); N, 12.3 (12.2). IR: ν (C═C, s) 1611, (V═O, s) 947, (O−O, s) 911, (V−O_2, s, as) 577, (ClO_4, s) 1090 cm^{-1}.

Physical and Spectroscopic Studies. Infrared spectra were recorded as KBr pellets on a Nicolet 60 SX Fourier transform spectrophotometer. UV/visible spectra were recorded on a Perkin-Elmer Lambda 9 spectrophotometer. NMR spectra were recorded using a Bruker 360 or 200 MHz instrument. ^{51}V NMR spectra were referenced to external neat $VOCl_3$ (0.0 ppm), ^{13}C NMR spectra were referenced to TMS (0.0 ppm) using the internal solvent peak or to DSS (0.0 ppm) in D_2O solvent, and ^{1}H NMR spectra were referenced to TMS (0.0 ppm) in d_3-acetonitrile. Mass spectral analysis was performed on a Finnegan GC−MS. Elemental analyses were performed by the University of Michigan Microanalysis Laboratory.

Reactivity and Kinetic Studies. All reactions were carried out in acetonitrile at room temperature. All reactions involving iodide were performed under an argon atmosphere in order to prevent the oxidation of iodide by atmospheric oxygen. Potassium salts of vanadium compounds were dissolved by the addition of 2 eq of 18-crown-6 for each potassium ion. Solutions used for kinetic measurements were maintained at a constant ionic strength by the addition of tetraethylammonium perchlorate. Reactions were initiated by addition of acid or acid/halide solutions. Reactions with half-lives of ≥5 min were recorded on a Perkin-Elmer Lambda 9 spectrophotometer at room temperature, and the resulting data were fitted using the curve-fitting software in the program Kaleidagraph. Reactions with half-lives ≤5 min were performed on an OLIS RSM-SF rapid scan−stopped flow system thermostated at 25.0 °C, and the resulting data were fitted using the software package provided with the OLIS RSM-SF. Initial rate data (≤5% of reaction) were fitted to a line using the general form $y = mx + b$, and reaction curves obtained under pseudo-first-order conditions were fitted to the general equation $y = a\exp(bx) + c$. Kinetic parameters were obtained from a plot of the observed rate data versus acid/buffer concentration and were fitted using the curve-fitting software in the program Kaleidagraph by generating a least squares fit to a general equation of the form $y = mx + b$. Bromination of Phenol Red was monitored by measurement of the absorbance at 595 nm for reaction aliquots which were extracted at specific time points and diluted into pH 7.1 phosphate buffer.

Collection and Reduction of X-ray Data. Suitable crystals of K[$VO(O_2)$Hheida] **(2)**, K[$VO(O_2)$ada] **(3)**, [$VO(O_2)$bpg] **(4)**, and H[$VO(O_2)$bpg]$_2$(ClO_4) **(6)** were obtained as described above and mounted in glass capillaries. Intensity data were obtained on a Siemens R3m/v or Syntex $P2_1$m/v diffractometer using Mo Kα radiation (0.710 73 Å) monochromatized from a graphite crystal whose diffraction vector was parallel to the diffraction vector of the sample. Three standard reflections were measured every 97 reflections. Crystal and data parameters are given in Table 1. Intensity data were collected using $\theta/2\theta$ scans. The data were reduced, the structure was solved, and the model was refined using the SHELXTL PLUS and SHELXL-93 program packages. Computations were carried out on a VAXstation 3500. In the subsequent refinement, the functions $\sum w(|F_o| - |F_c|)^2$ for **3** and $\sum w(|F_o^2 - F_c^2|)^2$ for **4** and **6** were minimized where $|F_o|$ and $|F_c|$ are the observed and calculated structure factor amplitudes. The agreement indices $R = \sum(|F_o| - |F_c|)/\sum|F_o|$ and $R_w = [\sum w(|F_o| - |F_c|)^2/\sum w|F_o|^2]^{1/2}$ for **3**, and $R1 = \Sigma||F_o| - |F_c||/\sum|F_o|$ and $wR^2 = [\sum w(F_o^2 - F_c^2)/\sum w(F_o^2)^2]^{1/2}$ for **4** and **6** were used to evaluate the results. Atomic scattering factors are from *The International Tables for X-Ray Crystallography*.[32] Hydrogen atoms were located on a difference Fourier map and allowed to refine isotropically. Unique data and final R indices

(32) *International Tables for X-Ray Crystallography*; Kynoch: Birmingham, England, 1974; Vol. 4.

Table 2. Selected Distances and Angles for $Na_2[VO(O_2)nta]\cdot 5H_2O$ (**1**),[a] $K[VO(O_2)Hheida]\cdot H_2O$ (**2**), $K[VO(O_2)ada]\cdot H_2O$ (**3**), and $[VO(O_2)bpg]\cdot H_2O$ (**4**)

	1[b]	**2**	**3**		**4**
			Distances (Å)		
V−O1	1.610(5)	1.601(1)	1.611(1)	V−O1	1.615(2)
V−O2	1.866(4)	1.865(1)	1.872(1)	V−O2	1.864(2)
V−O3	1.865(3)	1.864(1)	1.867(1)	V−O3	1.869(2)
V−O4	2.042(4)	2.051(1)	2.032(1)	V−N2	2.138(2)
V−O6	2.051(4)	2.038(1)	2.055(1)	V−N3	2.148(2)
V−O8	2.190(4)	2.236(2)	2.218(1)	V−O4	2.085(2)
V−N1	2.172(4)	2.194(2)	2.193(1)	V−N1	2.217(2)
O2−O3	1.433(6)	1.432(2)	1.438(2)	O2−O3	1.424(2)
			Angles (deg)		
O1−V−O2	104.3(2)	105.19(7)	103.65(5)	O1−V−O2	103.95(9)
O1−V−O3	105.1(2)	105.44(7)	106.01(5)	O1−V−O3	104.70(9)
O2−V−O3	45.2(2)	45.17(7)	45.24(5)	O2−V−O3	44.84(7)
O1−V−O4	95.3(2)	93.93(7)	94.40(5)	O1−V−N2	92.57(9)
O1−V−O6	93.4(2)	93.93(7)	93.62(5)	O1−V−N3	91.94(10)
O1−V−N1	90.8(2)	92.27(7)	91.81(5)	O1−V−N1	87.36(8)
O1−V−O8	167.0(2)	167.72(7)	166.94(5)	O1−V−O4	164.35(8)
O4−V−O6	149.2(1)	150.28(6)	150.39(4)	N2−V−N3	149.70(7)
O8−V−N1	76.8(1)	75.46(6)	76.68(4)	O4−V−N1	77.00(6)

[a] Da-Xu, W.; Xin-Jian, L.; Rong, C.; Mao-Chun, H. *Jiegou Huaxue (J. Struct. Chem.)* **1992**, *11*, 65−67. [b] Atom numbering modified to match that used in this manuscript.

are given in Table 1. Selected bond distances and angles for these compounds are provided in Table 2. Complete crystallographic details are given in Tables 1−6 of the supporting information.

Results

Description of Structures. The molecular structures of three new oxoperoxovanadium(V) complexes were determined by single-crystal X-ray diffraction methods. Crystallographic data are summarized in Table 1. Important bond lengths and angles are included in Table 2. The $Na_2[VO(O_2)nta]\cdot 5H_2O$ structure is known, and the related bond lengths and angles are included in Table 2 for comparison purposes. The structure of the potassium salt[28] of this complex has been reported; however, the complete structural data set has not been described in the literature. The structure of $K[VO(O_2)Hheida]\cdot H_2O$ **(2)** has been previously communicated.[27]

The structures of $[VO(O_2)Hheida]^-$ **(2)**, $[VO(O_2)ada]^-$ **(3)**, and $[VO(O_2)bpg]$ **(4)** that are shown in Figure 2 have a distorted pentagonal bipyramidal geometry with a terminal oxo in an axial position and a side-on bound peroxo group in the equatorial plane. The peroxo O−O bond lengths range from 1.424(2) to 1.438(2) Å and are essentially indistinguishable from the 1.43 Å average obtained for all of the previously characterized monoperoxovanadium(V) complexes.[33] The tertiary nitrogen is trans to the peroxo group in each complex. The ligand donor in the axial position trans to the oxo group is only weakly coordinated. Complex **2** varies from the others in this series by having a coordinated alcohol group in this position. The structure of **3** has a coordinated amide carbonyl oxygen bound trans to the terminal oxo, an indication of the oxophilic nature of vanadium(V).

$[VO(O_2)bpg]$ **(4)** and $H[VO(O_2)bpg]_2(ClO_4)$ **(6)**, shown in Figures 2C and 3, respectively, are inherently different from **1**, **2**, and **3** because the ligand donor sets are markedly altered. In these molecules a predominantly equatorial nitrogen ligation is seen. The carboxylate donor trans to the oxo group in **4** is more strongly bound than in **1**. This leads to a significant shortening of the trans oxygen distance (V1−O4 2.085 Å) compared with the neutral donors in **2** and **3**.

(33) Butler, A.; Clague, M. J.; Meister, G. E. *Chem. Rev.* **1994**, *94*, 625−638.

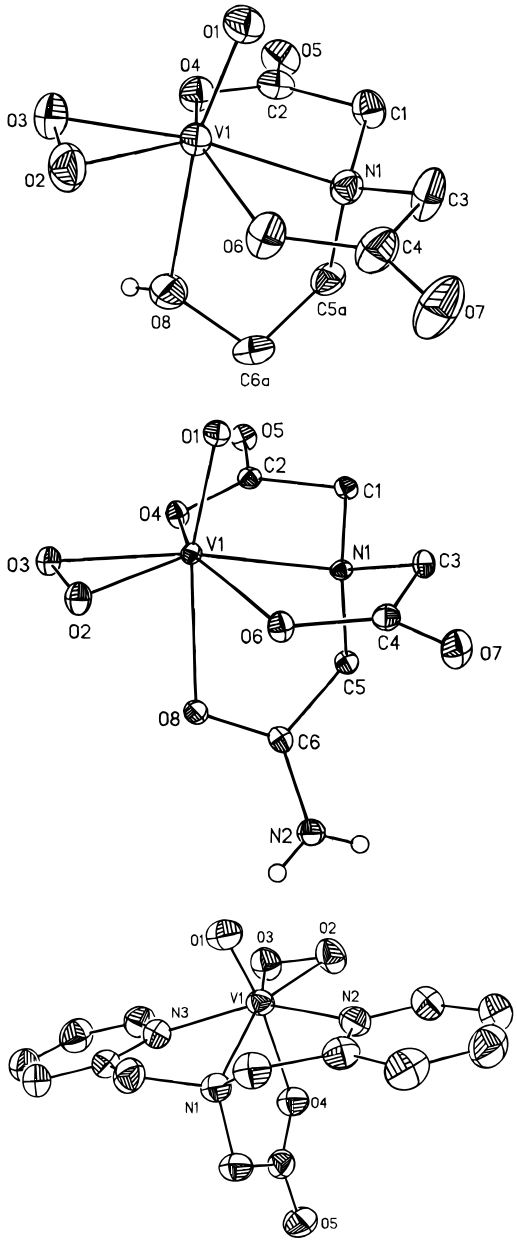

Figure 2. (A) ORTEP diagram of the $[VO(O_2)Hheida]^-$ (**2**) anion with thermal ellipsoids shown at 50% probability. (B) ORTEP diagram of the $[VO(O_2)ada]^-$ (**3**) anion with thermal ellipsoids shown at 50% probability. (C) ORTEP diagram of the $[VO(O_2)bpg]$ (**4**) molecule with thermal ellipsoids shown at 50% probability.

The structure of **6** is used here to determine atom connectivity only because of the poorly defined crystallographic model. It is likely that the high *R* value (0.0790) obtained is due to multiple conformations of the dimer within the unit cell. This appears to be confirmed by the observation of weak reflections associated with a supercell on a film exposure. The only distance observed in the structure consistent with a hydrogen-bonding interaction is that found between the nonchelated oxygen atoms of the carboxylate donor groups (2.44 Å), consistent with the placement of one proton per dimer as required to balance the charge of one perchlorate anion per dimer. We have included this structure report because of the general importance of this molecule as the only catalytically active protonated complex used in this study that has been crystallographically characterized.

Spectroscopic Characterization of Complexes. The metal−oxo (V═O) and peroxo (O−O) stretching modes were observed in the same region. The IR bands associated with each appear

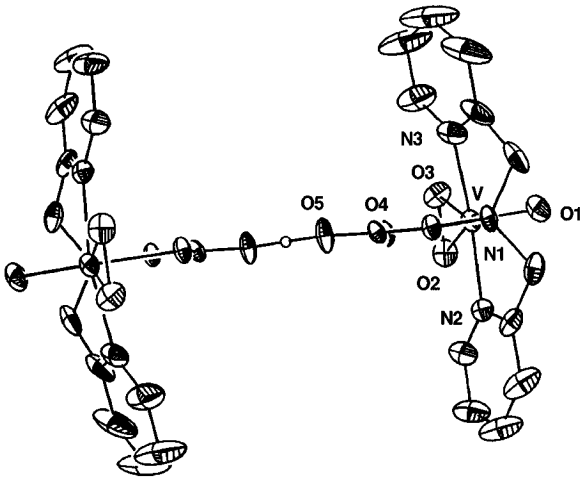

Figure 3. ORTEP diagram of the $H[VO(O_2)bpg]_2^+$ (**6**) cation with thermal ellipsoids shown at 50% probability.

to fall into two groups, depending upon the equatorial donors (e.g., 960 and 920 cm^{-1} for the bis(pyridyl)amine (**4** and **5**) vs 950 and 910 cm^{-1} for the bis(carboxylate)amine (**1**, **2**, and **3**) ligand types). Addition of a single equivalent of perchloric acid to **4** in acetonitrile did not make an observable difference in the positions of the vanadium−oxo (V═O) or peroxo (O−O) bands; however, the band at 1629 cm^{-1} associated with the carboxylate carbonyl (C═O) disappeared. This is consistent with the protonation of the carboxylate group as observed in the crystallographic analysis of **6**.

We have determined the identity of the bands associated with the peroxo group by isotopic substitution of the peroxo ligand of the Ba[$VO(O_2)$nta] complex using ^{18}O-enriched hydrogen peroxide. Two bands were observed to shift in the isotopically substituted sample. The peroxo (O−O) stretch moved from 920 to 870 cm^{-1}, and the vanadium−peroxo (V−O_2) stretch(es) moved from 563 to 542 cm^{-1}. The shifts obtained for the peroxo (O−O) stretching mode are close to the calculated value (52 cm^{-1}) expected upon ^{18}O substitution. The shift for the metal-peroxo band should be significantly less. The identification of these bands has allowed us to confirm the previous assignments for the peroxo group based on normal coordinate analysis.[34]

The properties of the species found in aqueous solution were explored using multinuclear NMR spectroscopy (Table 3). A single resonance is observed by ^{51}V NMR for each complex, within the range expected for monoperoxovanadium(V) complexes.[35] The coordination-induced shifts observed in the ^{13}C NMR spectra of the ligands upon binding to vanadate are well-defined in aqueous[36] and nonaqueous[37] solution and indicate tetradentate chelation for all of the ligands employed here, essentially the same as is observed in the solid state by crystallographic means. The ligand donors of the oxoperoxovanadium(V) complexes do not exchange on the NMR time scale in aqueous solution. The coordination of a peroxide appears to stabilize the ligand against rapid hydrolysis of the complex, even in aqueous solution at pH 4. This is in contrast to the exchange typically observed in vanadate complexes of aminocarboxylate ligands.[38] For example, the ^{13}C NMR of **1** gives two sets of carboxylate donor resonances which can be assigned as the axial and equatorial ligands; however, the dioxovanadium complex of nta only gives a single carboxylate resonance.

Table 3. Solution Spectroscopic Data for Oxoperoxovanadium Complexes

	Visible (nm)[a]				
	1	**2**	**3**	**4**[b]	**5**
H_2O	428 (350)	429 (330)	427 (420)	422 (270)	427 (270)
acn	447 (475)	447 (480)	451 (610)	444 (360)	437 (420)
	NMR (ppm)				
	H_2O			CH_3CN	DMSO
	1	**2**	**3**	**4**	**5**
^{51}V	−544	−565	−551	−545	−574
^{13}C	182.5	183.2	182.3	178.1	
	70.5	68.8	70.7	68.6	
	180.5	64.9	176.6	158.1	159.1
	68.8	59.9	66.7	147.7	147.1
				141.9	142.1
				126.5	125.8
				124.4	124.3
				68.8	67.8
					155.5
					146.1
					139.8
					123.8
					121.0
					64.4

[a] Extinction coefficient (M^{-1} cm^{-1}) given in parentheses after absorbance. [b] Dissolved with 1 equiv of perchloric acid.

The potassium salts of complexes **1**−**3** can be dissolved in acetonitrile upon addition of 18-crown-6. The UV/visible spectra of these compounds show a characteristic peroxo-to-vanadium charge transfer band at approximately 450 nm,[39] observed in both aqueous and nonaqueous solvents. **4** is reasonably soluble in acetonitrile as a neutral complex, but increases nearly 10-fold in solubility upon the addition of 1 equiv of perchloric acid. The ^1H NMR of **4** with 1 equiv of perchloric acid in acetonitrile gave a spectrum in which the pyridyl donors are equivalent, consistent with protonation of the axial carboxylate in solution.

Reactivity. In aqueous solution no reaction was observed with bromide at any pH at which the complex could be expected to remain intact. However, in acetonitrile solution these complexes rapidly oxidized both iodide and bromide upon the addition of perchloric acid. The reaction observed is as shown:

$$[VO(O_2)L] + H^+ + X^- \rightarrow [VO_2L] + \text{“}X^+\text{”} + OH^- \quad (1)$$

This species (“X^+”) is an equilibrium mixture of $HOX/X_2/X_3^-$, with the relative amounts determined by the acid/base and halide concentrations. The product observed by UV/visible spectroscopy is primarily tribromide or triiodide under the experimental conditions used here.

If an organic substrate capable of electrophilic aromatic substitution is present, the same reaction conditions used to oxidize halides can be used to perform halogenations. The overall reaction observed is as shown:

$$[VO(O_2)L] + H^+ + X^- + RH \rightarrow [VO_2L] + RX + H_2O \quad (2)$$

The reaction was followed by monitoring the visible conversion

(34) Griffith, W. P.; Wickens, T. D. *J. Chem. Soc. A* **1968**, 397−400.
(35) Rehder, D.; Weidemann, C.; Duch, A.; Priebsch, W. *Inorg. Chem.* **1988**, *27*, 584−587.
(36) Crans, D. C.; Ehde, P. M.; Shin, P. K.; Pettersson, L. *J. Am. Chem. Soc.* **1991**, *113*, 3728−3736.
(37) Colpas, G. J.; Hamstra, B. J.; Kampf, J. W.; Pecoraro, V. L. *Inorg. Chem.* **1994**, *33*, 4669−4675.
(38) Crans, D. C.; Shin, P. K. *Inorg. Chem.* **1988**, *27*, 1797−1806.
(39) Sivak, M.; Schwendt, P. *Transition Met. Chem. (London)* **1989**, *14*, 273−276.

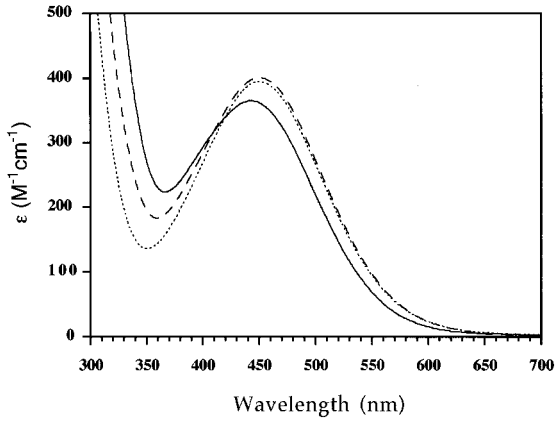

Figure 4. UV/visible spectra of the titration of perchloric acid into a 1.0 mM acetonitrile solution of [VO(O$_2$)bpg] (**4**) (solid line = 0 equiv of acid, dashed line = 1 equiv of acid, dotted line = 2 equiv of acid).

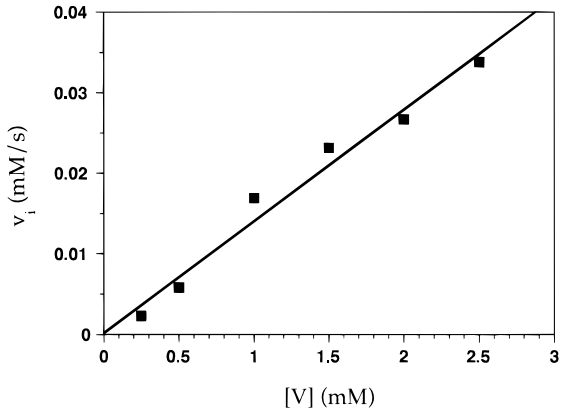

Figure 5. Initial rate dependence of bromide oxidation on the concentration of the vanadium complex H[VO(O$_2$)bpg](ClO$_4$) in acetonitrile (R = 0.9873). Conditions used: 25 mM TBABr, 25 mM TEAClO$_4$.

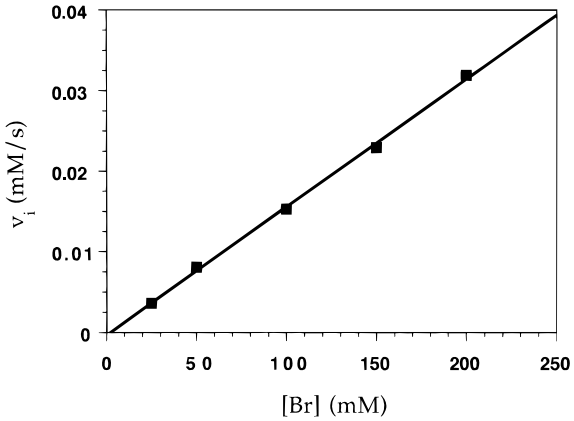

Figure 6. Initial rate dependence of bromide oxidation on the tetrabutylammonium bromide concentration for H[VO(O$_2$)bpg](ClO$_4$) in acetonitrile (R = 0.9992). Conditions used: 0.5 mM [VO(O$_2$)bpg], 0.5 mM HClO$_4$.

of Phenol Red to the tetrabrominated derivative Bromophenol Blue. No halogenation of the solvent or ligands has been detected.

In the absence of an organic substrate, dioxygen gas was generated upon the addition of an equivalent of hydrogen peroxide to a solution containing the oxidized halide species under basic conditions. Overall, the two reaction steps correspond to the halide-assisted disproportionation of hydrogen peroxide into water and dioxygen. The reaction observed is as shown:

$$[VO(O_2)L] + H^+ + H_2O_2 + OH^- \rightarrow [VO_2L] + O_2 + 2H_2O \quad (3)$$

This was confirmed by reaction of isotopically substituted peroxide ($H_2{}^{18}O_2$) with the oxidized halide solution. The only product observed by GC−MS sampling of the headspace is the isotopically enriched dioxygen ($^{18}O_2$). Mixing of isotopes was not observed in the dioxygen produced.

Each of these complexes catalyzed the bromination of Phenol Red in the presence of sufficient equivalents of peroxide, acid, and substrate, performing multiple turnovers in minutes at room temperature and millimolar concentrations. A control reaction containing all components except the vanadium complex also showed significant initial activity, but slowed as the reaction proceeded and reached completion in hours as opposed to minutes.

Mechanistic Studies. The addition of a proton to these complexes in acetonitrile solution produced observable changes in the UV/visible spectra. The addition of 1 equiv of perchloric acid to **4** was sufficient to cause a small shift in the peroxo-to-vanadium charge transfer band (Figure 4). The conversion to the protonated species was not cleanly isosbestic; however, the process was reversible. In contrast, the addition of 10 equiv of tetraethylammonium bromide in the absence of acid produced no observable change in the UV/visible spectra of these complexes.

The proton requirement for the halide oxidation reaction was determined. In the absence of an available proton no reaction was observed. Two equivalents of acid per vanadium complex was required to drive the halide oxidation reaction to completion based on peroxovanadium complex. This is consistent with eq 1; the second equivalent of acid is required to neutralize the hydroxide formed as a reaction product. However, in the presence of substrate, only 1 acid equiv was required to complete the bromination reaction. This is consistent with eq 2, as here the proton displaced upon halogenation is available to neutralize the hydroxide produced as a product of the halide oxidation step. Additional acid equivalents increased the rate of reaction. This acid dependence therefore precluded the examination of the bromide oxidation reaction as a pseudo-first-order kinetic process using the minimum number of acid equivalents; however, the initial rate method was utilized to provide mechanistic information.

The role of the vanadium complex in the halide oxidation reaction was investigated using **4**, which has the greatest solubility range in acetonitrile of the complexes studied here. The halide oxidation reaction was investigated in the presence of a single equivalent of perchloric acid by the initial rate method. When the initial rate was plotted against the concentration of peroxovanadium complex (Figure 5), a straight line was obtained. The slope of this line gave a pseudo-first-order rate constant of 0.014 s^{-1}, and a second-order rate constant of 0.14 M^{-1} s^{-1} when corrected for the bromide concentration. A plot of ln v_i vs ln [Br] for this data gave a straight line with a slope of 1.1, confirming the first-order dependence on vanadium.

Similar plots were generated for variations in bromide concentration. A straight line was also obtained from a plot of the initial rate dependence on the bromide concentration (Figure 6). The slope of this line gave a first-order rate constant of 1.6 $\times$ 10^{-4} s^{-1}, and a second-order rate constant of 0.16 M^{-1} s^{-1} when corrected for the concentration of the peroxovanadium complex. The values (k_1) obtained for the complexes under these conditions range from the low of 0.11 M^{-1} s^{-1} for **3** to a high value of 1.3 M^{-1} s^{-1} for **2** (Table 4). The reaction rate

Table 4. Kinetic Data for Halide Oxidation in Acetonitrile at 25 °C

complex (ligand)	k_{Br} (M^{-1} s^{-1})[a]	k_I (M^{-1} s^{-1})[b]	pK_a[c]	k_1 (M^{-1} s^{-1})[d]
1$^-$ (Hnta)	170 ± 30	1300 ± 300	6.0 ± 0.3	0.33 ± 0.05
2$^-$ (Hheida)	280 ± 40	1500 ± 300	6.0 ± 0.3	1.3 ± 0.3
3$^-$ (ada)	220 ± 30	1100 ± 500	5.8 ± 0.4	0.11 ± 0.03
4$^+$ (Hbpg)	21 ± 3	130 ± 30	5.4 ± 0.3	0.17 ± 0.08
5$^+$ (tpa)	100 ± 30		5.8 ± 0.4	0.22 ± 0.01
H_2O_2[e]	3.7 ± 0.9	340 ± 100	6.0 ± 0.4	0.23 ± 0.02

[a] Conditions used: 0.05 mM [$VO(O_2)$L], 5 mM $TEAClO_4$, 5 mM TBABr. [b] Conditions used: 0.05 mM [$VO(O_2)$L], 2.5 mM $TEAClO_4$, 2.5 mM TBAI. [c] Determined from plot of initial rate (v_i) vs acid/buffer concentration. [d] Conditions used: 0.5 mM [$VO(O_2)$L], 0.5 mM $HClO_4$, $TEAClO_4$, TBABr. [e] Anhydrous H_2O_2.

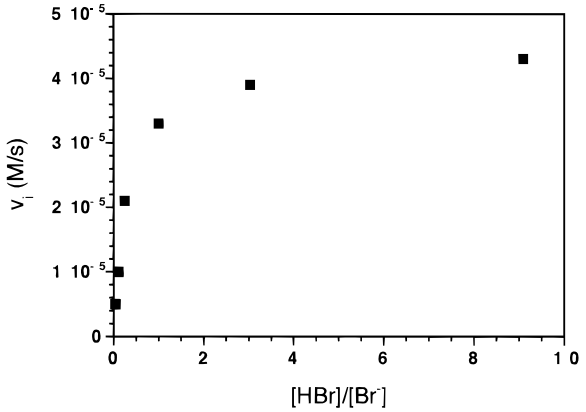

Figure 7. Initial rate dependence of bromide oxidation on the acid/buffer concentration for [$VO(O_2)$nta]$^{2-}$ (**1**) in acetonitrile. Conditions used: 0.05 mM [$VO(O_2)$nta]$^{2-}$, 25 mM TBABr, 25 mM $TEAClO_4$.

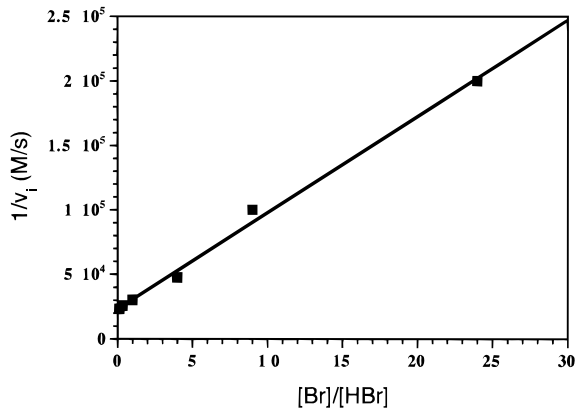

Figure 8. Determination of the maximum rate and pK_a of activation for bromide oxidation in acetonitrile by [$VO(O_2)$nta]$^{2-}$ (**1**) from plotting the inverse of the observed rate constant vs the buffer/acid concentration ratio ($R = 0.9973$). Conditions used: 0.05 mM [$VO(O_2)$nta]$^{2-}$, 25 mM TBABr, 25 mM $TEAClO_4$.

did not show signs of saturation kinetics with any complex used here even at concentrations of up to 0.25 M Br^-. A plot of ln v_i vs ln [Br] for this data gave a straight line with a slope of 0.97, confirming the first-order dependence on halide.

The role of the acid required for halide oxidation was further explored by kinetic studies of the peroxo complexes in the presence of additional equivalents of perchloric acid. The dependence of the initial rate of bromide oxidation on the acid/bromide concentration ratio is shown in Figure 7. A curve was obtained that approached a maximum rate of reaction at high acid/bromide concentration ratios. At higher acid/bromide ratios the time course of the reaction slowed considerably before the theoretical yield of product was obtained. A fit of this data indicates contributions consistent with the rates determined for the complex and free peroxide in solution. Hence only initial rates are used in kinetic determinations involving buffered solutions using more than 1 acid equiv per complex. This protonation reaction is particularly obvious for **5**, limiting the range of the kinetic fit.

Kinetic Models. The initial rate data obtained for the halide oxidation reactions using 1 equiv of a strong acid can be described by a model with the rate equation

$$\text{rate} = k[\text{HV}][\text{X}] \quad (4)$$

Here the protonated vanadium complex (HV) and the halide (X) are kinetically essential components.

Given that the halide oxidation reaction can be considered to be irreversible, there are three rate constants associated with this reaction:

$$\text{V} + \text{HA} \underset{k_{-1}}{\overset{k_1}{\rightleftharpoons}} \text{HV} + \text{A} \quad (5)$$

$$\text{HV} + \text{X}^- \xrightarrow{k_2} \text{products} \quad (6)$$

As proton transfer is generally a fast process relative to redox reactions (both k_1 and $k_{-1} \gg k_2$), this can be treated as a pre-equilibrium.

The steady state concentration of HV can be described under the initial rate conditions. Solving for [HV] and substituting into eq 4 gives the rate equation for the halide oxidation reaction under buffered conditions:

$$v_i = k_2[\text{X}](k_1[\text{HA}][\text{V}]/k_{-1}[\text{A}] + k_1[\text{HA}]) \quad (7)$$

This can be rearranged to give the rate equation written in the form of a line:

$$1/v_i = (1/K_{eq}k_2[\text{V}_t][\text{X}])([\text{A}]/[\text{HA}]) + 1/k_2[\text{V}_t][\text{X}] \quad (8)$$

where

$$K_{eq} = k_1/k_{-1} = [\text{HV}][\text{A}]/[\text{V}][\text{HA}] \quad (9)$$

Here $[V_t]$ is the total vanadium concentration in the reaction. Both K_{eq} and k_2 can be determined using a plot of $1/v_i$ versus [A]/[HA] as is shown in Figure 8. Using eq 9 we have obtained the effective pK_a for each complex given the pK_a of the buffer used. The rates and pK_a obtained from the halide oxidation reactions for each catalyst are given in Table 4.

Discussion

A series of oxoperoxovanadium(V) complexes was synthesized and characterized as models for the vanadium haloperoxidase enzymes. Various tripodal amine-based ligands were utilized, incorporating various combinations of carboxylate, alcohol, amide, and pyridine donors. These are similar to ligands previously employed to form stable peroxovanadium complexes[33] and were chosen to model some of the donor types considered likely to be found at the active site of the enzyme. The structurally characterized complexes all have a distorted pentagonal bipyramidal geometry which is typical of the peroxovanadium complexes previously studied.[33] The only complex used here which is not structurally characterized (**5**) also has spectroscopic and physical parameters consistent with the same basic structure.

Although these complexes were synthesized in water, they maintain the observed structural characteristics in both aqueous and nonaqueous solution. Complex **4** was recrystallized from acetonitrile solution giving the same basic structure as **1**, **2**, and **3** which were crystallized from water. In addition, the UV/

visible and multinuclear NMR data indicate that the structures observed in the solid state appear to be conserved in solution. The peroxo group appears to play a key role in stabilizing these complexes as it reduces the ligand hydrolysis commonly observed for vanadate complexes.

The structure of a partially protonated form of complex **4** was obtained, and the proton was found to be bridging between the axial carboxylate groups to form a dimer of complexes in the solid state. The location of the proton as being bound to the nonchelated carboxylate oxygen in the structure of **6** can also be inferred using infrared data. The ^{1}H NMR spectrum of **4** with 1 equiv of perchloric acid in acetonitrile is consistent with carboxylate protonation in solution, as indicated by solid state studies of **6**. This may also be the case for acid solutions of the other complexes which have axial carboxylate, pyridyl, and amide groups which can be protonated, but not for **2** which has an alcohol group in this position.

In aqueous solution these complexes do not react with bromide above pH 2−3, at which point the species present would likely include some of the various peroxovanadates shown to catalyze the oxidation of bromide at acidic pH. In acetonitrile the complexes studied here will oxidize both iodide and bromide in the presence of any sufficiently acidic proton source. The reason for this solvent dependence is due to the buffering ability of water, which can prevent protonation of the complex. In aqueous solution the approximate pK_a which would be estimated for these complexes is near 0, a value based on the known aqueous pK_as for the protonation of different functional groups on several indicator dyes having a pK_a near 6 in acetonitrile.[40] This would explain the lack of reactivity under aqueous conditions at any pH at which a complex would be expected to remain intact. Additionally, the presence of a millimolar concentration of water in acetonitrile does not appear to have any effect on the reaction. The pK_a of hydronium ion in acetonitrile is 2.3; therefore, a very high concentration of water would be necessary to act as an effective buffer.

Halogenation was measured using the visible conversion of Phenol Red to Bromophenol Blue, a commonly used assay for haloperoxidase activity in enzymes.[5] The stoichiometry of the reaction, given sufficient acid and bromide, approaches a maximum of one bromination per peroxovanadium(V) complex. This bromination appears to occur only at an activated position on an aromatic ring and has not been observed to occur with an aliphatic substrate or any of the ligands used here. This is consistent with a mechanism involving the oxidation of the halide by two electrons, and not with a one-electron or radical mechanism of oxidation.

When multiple equivalents of hydrogen peroxide, halide, and acid are present, these complexes act as catalysts for the peroxidative halogenation of an organic substrate. Multiple brominations of Phenol Red are completed within minutes. The catalytic halogenation reaction observed is shown below:

$$[VO(O_2)L] + X^- + H^+ \rightarrow [VO_2L] + \text{“}X^+\text{”} + OH^-$$

$$RH + \text{“}X^+\text{”} + OH^- \rightarrow RX + H_2O$$

$$\underline{[VO_2L] + H_2O_2 \rightarrow [VO(O_2)L] + H_2O}$$

$$RH + H_2O_2 + HX \rightarrow RX + 2H_2O$$

The summation obtained here is the balanced equation as written for the vanadium haloperoxidase enzyme. Each of these reaction steps can be independently observed with the complexes used in this study.

In the absence of an organic substrate, the solution containing the oxidized halogen species will generate dioxygen with the addition of a single equivalent of both hydrogen peroxide and base. This reaction does not occur under acidic conditions and is likely due to the generation of HOBr upon the addition of base which will undergo this well-characterized reaction with hydrogen peroxide.[41] This reaction has been proposed to occur with the enzyme, which has been observed to generate singlet oxygen. Singlet oxygen is also produced by reaction with HOI, but is immediately quenched by excess iodide and not easily observed.

Using the chemistry observed here the reactions for a catalytic halide-assisted disproportionation of hydrogen peroxide[42] can be written as shown:

$$[VO(O_2)L] + X^- + H^+ \rightarrow [VO_2L] + \text{“}X^+\text{”} + OH^-$$

$$H_2O_2 + \text{“}X^+\text{”} + 2OH^- \rightarrow O_2 + X^- + 2H_2O$$

$$\underline{[VO_2L] + H_2O_2 \rightarrow [VO(O_2)L] + H_2O}$$

$$2H_2O_2 + H^+ + OH^- \rightarrow O_2 + 3H_2O$$

The summation written here is simply the disproportionation of hydrogen peroxide with the generation of an extra water of neutralization in the production of HOX. This reaction does not turn over under these conditions but can be cycled by the sequential addition of hydrogen peroxide, acid, and base.

The model system developed here can be used to probe the active oxidant formed upon protonation of the complex. The addition of 1 equiv of perchloric acid to these complexes in acetonitrile solution produces observable spectroscopic changes consistent with the protonation of one or more sites on the complex. The absence of a clean isosbestic point may indicate that the complexes undergo measurable degradation in the time scale of the titration, which would be consistent with the reversible behavior of the remaining complex upon addition of base. This implies that protonation of these complexes proceeds without any major structural rearrangement.

While the kinetics obtained indicate that the halide oxidation reaction is first order in both peroxovanadium complex and halide, the actual amount of acid required to achieve the maximum rate is pK_a and concentration dependent. Bromide is capable of acting as a buffer with a pK_a of 5.5 in acetonitrile,[43] and it is protonated by perchloric acid. When the initial rate of halide oxidation was plotted against the hydrohalic acid/halide ratio, a curve was obtained that plateaus at a maximum initial rate. This maximum rate corresponds to the complete activation of the peroxovanadium complex by protonation. Therefore, an equation involving a fast pre-equilibrium and then a rate-determining second-order reaction was used to describe the observed kinetics. A linear equation was generated and the initial rate data was fitted to give both K_{eq} for the protonation equilibrium and k_x for the maximum rate of halide oxidation from the slope and intercepts.

The rates obtained for bromide and iodide oxidation by each of the complexes studied here are given in Table 4. Variation of the ligand donor set leads to significant differences in the efficiency of halide oxidation. The complexes formed with the

(40) Kolthoff, I. M.; Chantooni, M. K., Jr.; Bhowmik, S. *Anal. Chem.* **1967**, *39*, 315−320.
(41) Cahill, A. E.; Taube, H. *J. Am. Chem. Soc.* **1952**, *74*, 2312−2318.
(42) Espenson, J.; Pestovsky, O.; Huston, P.; Staudt, S. *J. Am. Chem. Soc.* **1994**, *116*, 2869−2877.
(43) Izutsu, K. *Acid-base Dissociation Constants in Dipolar Aprotic Solvents*; Blackwell Scientific Publications: Oxford, 1990.

Scheme 1

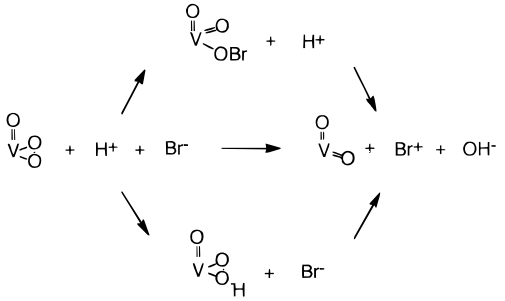

bis-carboxylate type ligands are clearly shown to be more efficient catalysts for both bromide and iodide oxidation. The rate obtained for the fastest catalyst, **2**, is within 2−3 orders of magnitude of the maximum bromination rates obtained for the enzyme, depending on the source of the enzyme studied.[21]

The reason for the difference in rate between the two sets of ligands is not clear. However, there is a significant range in overall charge between the complexes, from −2 for **1** to +1 for **5** and **4** (if fully protonated), which roughly corresponds with the faster and slower rates obtained for the oxidation, respectively. This is also reflected in the pK_as obtained, with the more negatively charged complexes being more basic. As proton transfer is not the rate-determining step for halide oxidation, the overall charge on the protonated complex may be relevant.

The limiting forms for the potential mechanistic pathways consistent with the kinetic data obtained for this reaction are shown in Scheme 1. The presence of excess bromide does not cause any observable change in the visible spectrum of these complexes, indicating that the pathway in which halide reacts first is unlikely. In contrast, the presence of a single equivalent of a sufficiently strong acid produces a small but observable change in the UV/visible spectra of these complexes. The rate of proton transfer is generally quite rapid and can be treated as a pre-equilibrium in the overall rate equation. This is consistent with viewing the protonation step as necessary for activation of the peroxo complex, although it is still not inconsistent with a concerted reaction mechanism.

The most likely group to be protonated upon activation of the complex is the peroxo. A protonated form of an oxodiperoxovanadium(V) complex has been crystallographically characterized.[44] The proton was found to bridge the peroxo groups of two complexes to form a dimer. Protonation of the peroxo increases the asymmetry observed in the V−O_{peroxo} bonds as compared to the unprotonated examples. This asymmetry is also observed in a vanadium alkyl/peroxide structure,[45] which should be electronically similar to the protonated form of the monoperoxo complexes used here.

Heterolytic cleavage of the peroxide O−O bond could be assisted by generation of a side-on bound hydroperoxide. Protonation could serve to activate the peroxide toward reaction with halide by causing asymmetry in binding to vanadium and/or by neutralizing the charge on one of the peroxo oxygens. The formation of a partial positive charge on the protonated peroxide oxygen would assist attack by the negatively charged halide ion and be consistent with an oxo-transfer mechanism for halide oxidation. The proposal for a vanadium−peroxide complex acting as an oxo-transfer agent also has literature precedent.[46]

(44) Szentivanyi, H.; Stomberg, R. *Acta Chem. Scand.* **1984**, *A38*, 101−107.

(45) Mimoun, H.; Chaumette, P.; Mignard, M.; Saussine, L.; Fischer, J.; Weiss, R. *Nouv. J. Chem.* **1983**, *7*, 467−475.

(46) Ghiron, A. F.; Thompson, R. C. *Inorg. Chem.* **1990**, *29*, 4457−4461.

Scheme 2

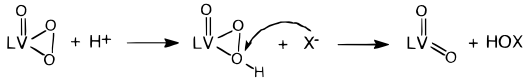

Scheme 3[a]

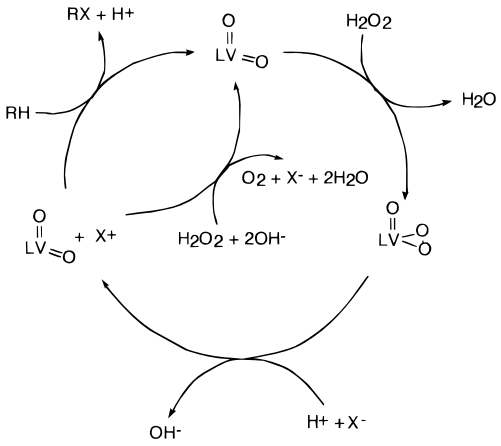

[a] X^+ = (Enz−X^+, V−OX^+, HOX = X_2 = X_3^-).

The mechanism for the halide oxidation reaction proposed for the series of complexes studied here involves nucleophilic attack by the halide on the protonated peroxo ligand of the complex, resulting in oxo transfer with simultaneous two-electron transfer as shown in Scheme 2. This is depicted for the generalized case of reaction with halide to form hypohalous acid as the product. In the enzyme a suitable acid/base catalyst would be needed at the active site to generate this intermediate.

The basis for the pH dependence of the halogenation and oxygen production reactions observed for the enzyme is explainable by examination of the two summations given above. The halogenation reaction cycle requires a proton and is the favored pathway for the enzyme at a more acidic pH, whereas the oxygen production cycle also requires the addition of a basic equivalent in the second step and is favored by more a basic pH in enzyme studies.

Although the structure of the vanadium active site in the structurally characterized inactive form of the vanadium chloroperoxidase appears not to be identical to any of the compounds used in this study, the general lessons learned from this system may be applied to the enzyme. A catalytic cycle can be proposed for the vanadium haloperoxidase enzyme based on this work, shown in Scheme 3. This catalytic cycle is consistent with all of the currently known features of the enzymes' reactivity and mechanism. The acid/base requirements for each step of the cycle are given in terms of H^+ or OH^-, although an acid/base catalyst(s) is likely to be located at the active site to perform this function in the enzyme. The species generated by the oxidation of the halide is given as X^+ to indicate one or more of the possibilities given.

The oxidized halide species observed under our reaction conditions is triiodide or tribromide, but should initially be hypohalous acid. This may also be the case for the enzyme; however, this could be used to generate an enzyme-bound hypohalite or halo-nitrogen species *in vivo*, which would then act as the actual halogenating agent. An enzyme-bound species has been proposed as a means of performing site-selective halogenation.[6]

Conclusions

In summary, a series of oxoperoxovanadium(V) model complexes were characterized as functional models for the

vanadium haloperoxidase enzymes. These complexes are shown to have reactivity which reproduces the peroxidative halogenation and halide-assisted peroxide disproportionation reactions as observed for the enzyme. In addition, some of these complexes are shown to be efficient halogenation catalysts under turnover conditions. Each step in the catalytic cycle has been independently characterized. This allowed us to determine the kinetic details of the halide oxidation reaction and determine the bimolecular rate constants for both bromide and iodide oxidation. A proton is consumed in each oxidation and is required for activation of the peroxovanadium complex in a pre-equilibrium step for which the relevant pK_a was determined. Based on the chemistry observed for our complexes we have proposed a mechanism for the halide oxidation reaction and a stepwise catalytic cycle for the enzyme. Also, the conditions under which halogenation occurs in our model systems may indicate the presence of a hydrophobic active site with a nearby acid/base catalyst in the vanadium haloperoxidase enzyme. Just such an environment appears to be present, based on the crystallographic analysis.[18]

Acknowledgment. Financial support from the National Institutes of Health (Grant GM 42703) is gratefully acknowledged.

Supporting Information Available: ORTEP figures with complete numbering schemes, tables of crystal data and structure refinement details, tables of fractional atomic coordinates with equivalent isotropic displacement parameters, a complete set of bond distances and angles, anisotropic thermal parameters, fractional atomic positions for hydrogen atoms, and tabulated kinetic data for **3**, **4**, and **6** (31 pages). This material is contained in many libraries on microfiche, immediately follows this article in the microfilm version of the journal, can be ordered from the ACS, and can be downloaded from the Internet; see any current masthead page for ordering information and Internet access instructions.

JA953791R